Time-Dependent Changes in Mechanical Properties of Neat and Reinforced Epoxy Resins

JOVAN MIJOVIĆ, *Department of Chemical Engineering, Polytechnic Institute of New York, Brooklyn, New York 11201*

Synopsis

Several neat and reinforced epoxy resin formulations were prepared and investigated. Solid glass microspheres, with and without coupling agent, were used as reinforcement. After completion of post-cure all samples were quenched into an ice-water bath. Upon removal from the ice-water bath, dynamic mechanical and fracture properties of all samples were evaluated as a function of time elapsed after quenching. Electron microscopic evidence was obtained for the existence of nodular morphology in all cured systems. The changes in dynamic mechanical and fracture parameters, induced by the sub-T_g annealing, were described in terms of the model of inhomogeneous thermoset morphology.

INTRODUCTION

During the final stage of processing, polymers are solidified by either cooling from the melt (thermoplastics) or by curing (thermosets). Often, processing operations include the quenching of a polymer to a temperature (T) below its glass transition (T_g). It is generally assumed that, as long as the polymer remains at $T < T_g$, its morphology will not change as a function of time. However, it has been known for some time that various quenched thermoplastic polymers exist in a nonequilibrium state and that time-dependent variations in their physical properties occur, even at temperatures below the glass transition.[1-9] On the molecular level, the tendency of polymeric chains to reach an equilibrium conformation is reflected in an increase in density or a decrease in free volume of the polymer. The magnitude of molecular motions in the glassy state increases as the temperature approaches the T_g and/or in the presence of an aggressive environment, such as applied stress or an organic solvent. The molecular motion in the solid state in the absence of an aggressive environment has created considerable interest among polymer scientists and engineers and is discussed in this study.

It wasn't until recently, however, that such time-dependent changes in physical properties have been reported in highly crosslinked thermosets. For instance, various epoxy and polyester resins were found to undergo structural rearrangements in the laboratory at room temperature.[10-14] Since the latter is well below the T_g of highly crosslinked thermosets, this phenomenon has been commonly referred to as the "sub-T_g annealing." As a direct consequence of such molecular rearrangements in the glassy state, the thermomechanical properties of these polymers have been reported to change, although no explanation in terms of the polymer morphology has been offered.

In neat thermosets, the extent of sub-T_g annealing is primarily determined by the frozen-in stresses, introduced into the system via the thermal gradients

Journal of Applied Polymer Science, Vol. 27, 2919–2931 (1982)
 CCC 0021-8995/82/082919-13$02.30

TABLE I
Chemical Structure of Epoxy Resin and Curing Agent

(a) Typical diglycidyl ether of bisphenol A (DGEBA) resin:

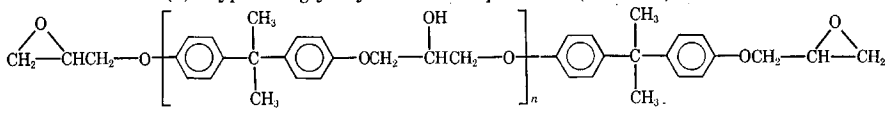

(b) Diethylene triamine (DETA) curing agent:

$H_2N—CH_2—CH_2—NH—CH_2—CH_2—NH_2$

which exist during cooling. The phenomenon of sub-T_g annealing is even more complex in thermoset matrix composites, where additional stresses develop in quenched samples due to the difference in thermal conductivities of the reinforcement and the matrix. Hence, the objective of this study was to investigate the time dependence of physical properties of a neat epoxy resin and two glass-reinforced composites, quenched and subsequently sub-T_g annealed. The surface of one glass reinforcement was treated with a coupling agent in order to investigate its role (if any) during molecular rearrangements in the glassy state.

Molecular motions in the glassy state and their effect on thermomechanical properties of samples as a function of time are best described by dynamic mechanical and fracture measurements. The former are known to be particularly sensitive to various structural heterogeneities, morphological gradients, and interphases. Fracture measurements, on the other hand, are sensitive to the presence of residual stresses whose magnitude is expected to change, due to molecular rearrangements, as a function of time.

EXPERIMENTAL

Chemical Systems

Resin of Epon 825, Shell's liquid diglycidyl ether of bisphenol A (DGEBA), a purified form of commercially available Epon 826, was cured with diethylene triamine (DETA). The chemical structure of resin and curing agent is shown in Table I. Potters Industries, Inc. glass microspheres were used as reinforcement. Composition and cure schedule of epoxy systems are described in Table

TABLE II
Various Formulations Studied

Formulation or system no.	Composition	Type of surface treatment on reinforcement	Cure schedule
1	Epon 825 + 11 phr DETA		24 h at RT + 4 h at 128°C
2	Epon 825 + 11 phr DETA + 25 phr (by wt) glass spheres # 3000	None	Same as 1
3	Epon 825 + 11 phr DETA + 25 phr (by wt) glass spheres # 3000 CP-02	Coupling agent recommended for use with epoxies	Same as 1

TABLE III
Schedule[a] for Dynamic Mechanical and Fracture Measurements

	System no.	Sample no. 1	2	3	4	5	6	7	8	9	10
		Time (h)									
DMA	1	0.15	1	3	5	15	38	90	216	744	1224
	2	0.50	1	3	5	15	38	72	216	744	1224
	3	0.45	1	3	5	15	38	83	216	744	1224
Fracture tests	1	0.33	1	3	5	10	20	72	168	672	1080
	2	0.33	1	3	5	10	20	72	168	672	1080
	3	0.33	1	3	5	10	20	72	168	672	1080

[a] Each entry represents the time (h) elapsed between the moment the sample was removed from ice-water bath and the moment the test was begun.

II. Immediately after post-cure, samples were quenched in an ice-water bath and maintained there for 15 min. Next, all samples were removed from the quench bath and tested at time intervals described in Table III.

Techniques

Specimens for dynamic mechanical measurements were cast in silicone rubber molds. A Silastic E RTV rubber (Dow Corning) cured with 10 parts per hundred parts of resin, by weight (phr) of Silastic E curing agent was used for the preparation of molds. Weight changes as a function of immersion time were determined with an analytical balance (Mettler Instrument Corp.). Dynamic mechanical measurements were performed in DuPont 981 DMA module connected to 1090 Thermal Analyzer. All tests were run at the oscillation amplitude of 0.2 mm peak-to-peak and heating rate of 5°C min.

Linear elastic fracture mechanics (LEFM) analysis was applied to calculate the fracture energy of samples prepared in the form of adhesive joints. Width-tapered double cantilever beam (WTDCB) specimens, used for fracture energy measurements are described in Figure 1. By tapering the specimen width, the strain energy release rate (G_i) becomes independent of the crack length.

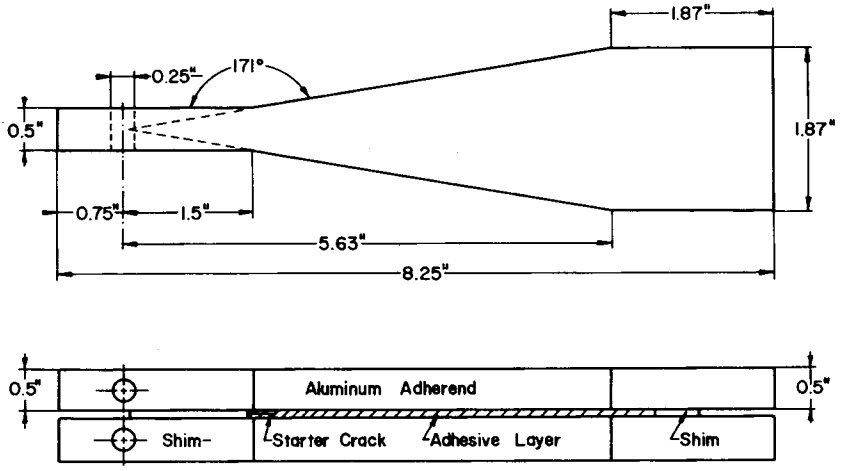

Fig. 1. Width tapered double cantilever beam (WTDCB) specimen for mode I fracture testing.

Preparation of surfaces of WTDCB specimens is described in Table IV. The subsequent application of resin on the beams has been detailed elsewhere.[15] An Instron Tensile Tester was used for fracture measurements, at room temperature and a crosshead speed of 0.127 cm/min (0.05 in./min).

One-stage carbon–platinum (C—Pt) replicas of fracture surfaces were made and studied by transmission electron microscopy (TEM). A detailed description of the sample preparation method is given elsewhere.[16] A Philips EM 200 model transmission electron microscope was used to investigate the fracture surfaces.

RESULTS AND DISCUSSION

Optimum mechanical properties of a cured thermoset are achieved when its glass transition reaches a temperature ($T_{g\infty}$) above which no further curing reactions take place, and such a thermoset network is then said to be fully cured. There are two molecular phenomena encountered during thermoset cure, namely gelation and vitrification, whose interrelation has been extensively discussed by Gillham.[17] In the case of crosslinked thermosets, one must realize that as long as the temperature of cure (and/or post-cure) remains below $T_{g\infty}$, vitrification will prevent completion of chemical reactions and such networks will not be fully cured. The T_g of an incompletely cured network will depend on the highest temperature achieved during cure (and/or post-cure), and, hence, optimum mechanical properties will not be developed. Many studies of thermosets reported in the literature have overlooked or simply left out this important fact.

TABLE IV
Procedure for Cleaning of Aluminum Beams Prior to Application of Adhesive

1. *Solvent treatment*
   a. Ethyl alcohol—removes blueing
   b. Perchloroethylene—removes grease, fingerprints, oil
2. *Alkaline treatment*
   "Oakite" #164, 449 g in 6000 mL of deionized water at 180 ± 5°F (82 ± 3°C) for 15 min followed by immediate water rinse (5 min)
3. *FPL Etch*
   165 g $Na_2Cr_2O_7$, 895 mL H_2SO_4, 4940 mL distilled water at 150 ± 5°F (66 ± 3°C) for 15 min followed by immediate water rinse (5 min)
4. *Phosphoric acid anodize bath*
   600 mL H_3PO_4 (85% ortho, sp gr = 1.436 g/cm^3) in 5400 mL water at 65–85°F (18–29°C) for 20–25 min at an applied potential of 10 ± 1 V, followed by a cold water rinse (within 2 min) for 10–15 min
5. *Drying*
   Blow off the water (with air), dry the beams by hanging them up with stainless steel wire; prime within 3 h
6. *Priming*
   BR-127 corrosion inhibiting adhesive primer (a modified epoxy phenolic primer manufactured by American Cyanamid Co.); warm primer to room temperature, mix thoroughly, continuously agitate during application. Spray to a primer thickness of 0.0001–0.0004 in. Good results have been obtained using a Devilbiss Spray Gun with Fluid Needle MBC-44F, Fluid Tip AV-15F, and Air Cap #36. Airline pressure of 40 psi is satisfactory. Air dry for 30 min, oven cure for 60 min at 250°F (121°C). Clean the primed surfaces with acetone prior to the application of the adhesive.

Consequently, in the first series of experiments, designed to establish a set of reference conditions, post-curing was done at various elevated temperatures, and the $T_{g\infty}$ of the system (as defined by the location of loss modulus peak in dynamic mechanical spectra) was found to be $\leq$128°C. In order to develop optimum mechanical properties in fully cured systems, in addition to post-curing at $T \geq T_{g\infty}$ (128°C) one must determine the minimum post-curing time needed to reach $T_{g\infty}$. The value of T_g increased during the first 4 h of post-cure at 128°C and then began to drop. Hence, post-cure time of 4 h and post-cure temperature of 128°C were chosen as optimal processing conditions, and have been used throughout this study. The glass transition of each specimen will be hereafter defined by the location of loss modulus peak (E'') in the dynamic mechanical spectrum.

We begin our discussion by considering dynamic mechanical properties of all systems. Changes in glass transition (T_g) and secondary transition (T_β) as a function of annealing time are shown in Figures 2–4, for formulations 1, 2, and 3, respectively. Several interesting observations have been made. At any given annealing time, the value of T_g shows insignificant dependence upon the presence of filler, with and/or without the coupling agent. Generally, it is believed that the T_g can either increase or decrease upon the addition of a filler, depending on the factors such as absorption[18] and the degree of agglomeration of filler particles.[19] It is further seen in Figures 2–4 that all three formulations display a similar pattern, in that the T_g gradually decreases as a function of annealing

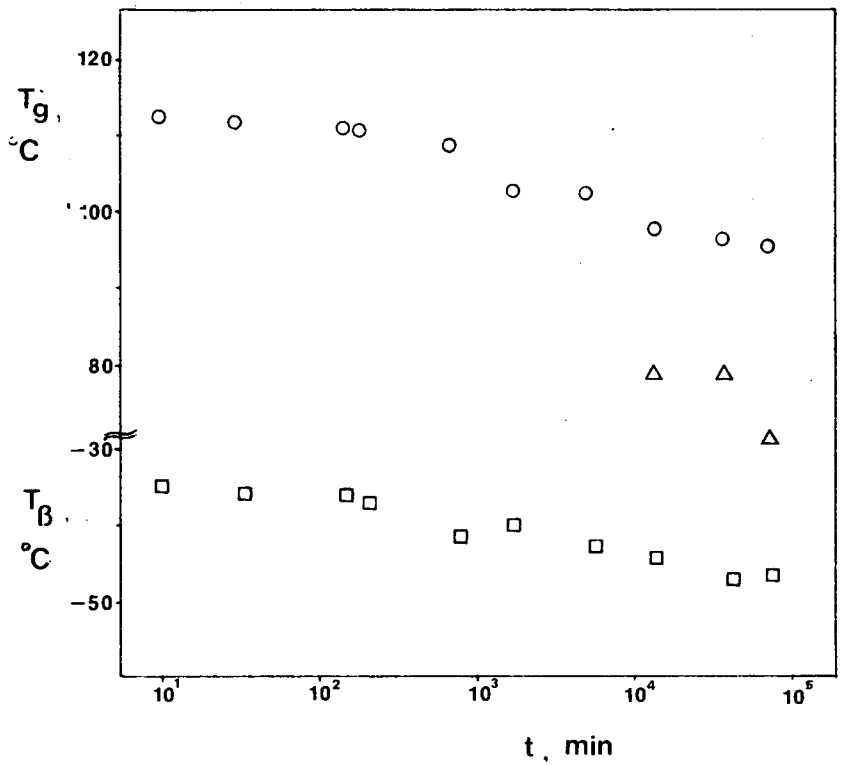

Fig. 2. Glass transition and secondary relaxations as a function of annealing time for formulation 1: (○)T_g; (△)T_g^1; (□)T_β.

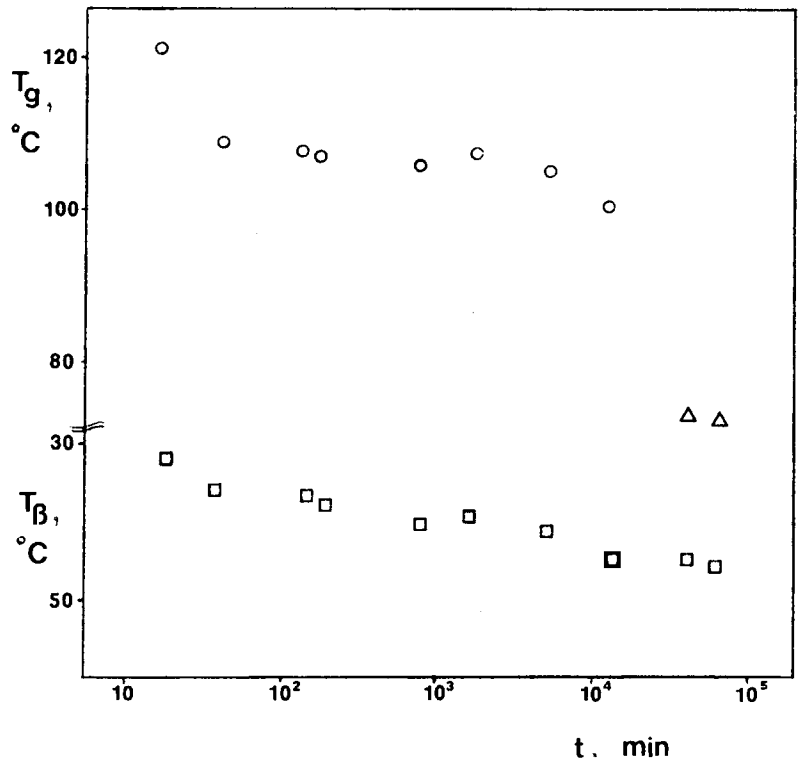

Fig. 3. Glass transition and secondary relaxations as a function of annealing time for formulation 2: (○)T_g; (△)T_g^1; (□)T_β.

time. After several days of annealing, two overlapping peaks start to appear in the T_g region of all formulations. We believe that such behavior is a direct consequence of the existence of inhomogeneities in thermoset morphology. For a long time, the concept of one indefinitely large (giant) molecule, forming a homogeneous network, has been used to describe the morphology of crosslinked thermosets. However, an apparent inadequacy of such morphological model in explaining various properties of thermosets, together with the ample experimental evidence collected within the last two decades, have led to a formulation of the concept of inhomogeneous thermoset morphology. It is generally recognized today that the model of higher crosslink density regions immersed in a lower crosslink density matrix most adequately describes the morphology of thermosets.[20]

A sudden quenching from the post-cure temperature to a temperature well below the T_g introduces a certain amount of frozen-in stresses in the sample. In terms of the inhomogeneous thermoset morphology, the majority of these stresses are induced in the regions of lower crosslink density, where the molecular motions of polymeric chains are less restricted (hindered). Some chains, or portions thereof, are "trapped" during sudden quenching and, from the thermodynamic point of view, exist in a nonequilibrium conformation. Since the T_g is determined (in dynamic mechanical measurements) through the response of a sample to cyclical stress, all specimens which contain internal (frozen-in) stresses, appear stiffer to any additional stress (deformation). Consequently, the onset of mo-

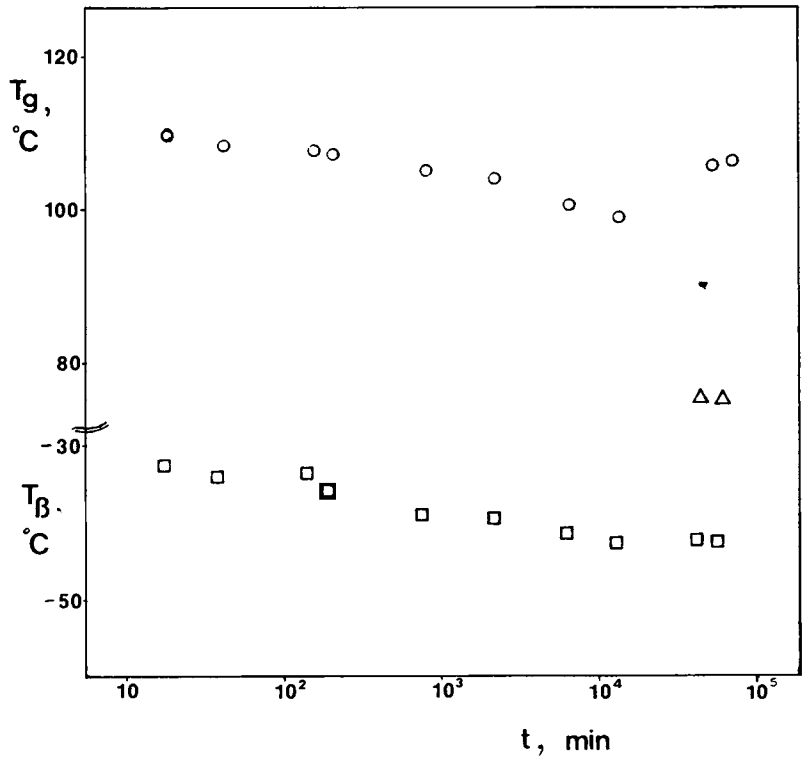

Fig. 4. Glass transition and secondary relaxations as a function of annealing time for formulation 3: (○)T_g; (△)T_g^1; (□)T_β.

lecular motion (T_g) in those specimens is shifted to a higher temperature. As a function of annealing time, however, the existing nonequilibrium state is altered by the molecular rearrangements which occur in the glassy state (and hence very slowly). On the morphological level, such transformations (referred to as the sub-T_g annealing) are believed to lead to the formation of a more closely packed and aligned matrix. A schematic description of this process is shown in Figure 5. This "ordering" (not separation) of the less highly crosslinked matrix is achieved by the small scale molecular motions and should not be referred to as the "phase separation." The electron density difference between these two regions is very small. For instance, small angle X-ray scattering (SAXS) measurements were unsuccessful in distinguishing between the two regions.

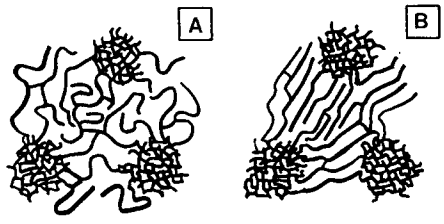

Fig. 5. A schematic representation of molecular rearrangements in the less highly crosslinked regions during the sub-T_g annealing (A) immediately after quenching and (B) after several weeks.

The driving force for these molecular rearrangements is the tendency of chains to move in the direction of a relief of frozen-in stresses. Since the sample which contains a reduced amount of frozen-in stresses appears less stiff to additional small stresses (deformations), applied during dynamic mechanical testing, the onset of molecular motion (T_g) shifts to a lower temperature, as seen in Figures 2–4. At this junction we note that our results do not agree with findings of Ophir and co-workers.[11] These authors reported that the T_g of the annealed samples was somewhat higher than in the quenched state, although neither a plot of T_g as a function of annealing time nor an explanation of morphological changes during annealing causing the increase in T_g, have been advanced. Also, the experimental techniques used in their study, namely DSC and tensile testing, are inferior to dynamic mechanical measurements with respect to the sensitivity to molecular relaxations in the solid state.

Eventually, the molecular rearrangements in the less highly crosslinked regions will have taken place to an appreciable extent (as qualitatively described in Fig. 5), and will become detectable by dynamic mechanical measurements. An indication of this molecular process is the appearance of a shoulder in the loss modulus (E'') spectra, after approximately 1 week. The development of the shoulder as a function of annealing time, is clearly seen in Figures 6–8, for formulations 1, 2, and 3, respectively. On the molecular level, this shoulder signifies the presence of another type of molecular relaxation which occurs at a temperature hereafter referred to as the T_g'. That relaxation, we believe, corresponds to the loss of order in less highly crosslinked regions achieved during the sub-T_g annealing. The peak that follows T_g' represents the onset of molecular motions in the more highly crosslinked regions which have been shown previously to be instrumental in determining the T_g of the sample.[21] Naturally, once the sample is heated to above its T_g, the order achieved during the sub-T_g annealing is lost.

In this study, samples were quenched into an ice bath in order to enhance the possibility of chains being "trapped" in a nonequilibrium conformation and hence facilitate the observation of ensuing molecular rearrangements. It should be noted, however, that the time-dependent changes in mechanical properties have also been observed in thermosets quenched to the ambient temperature. A

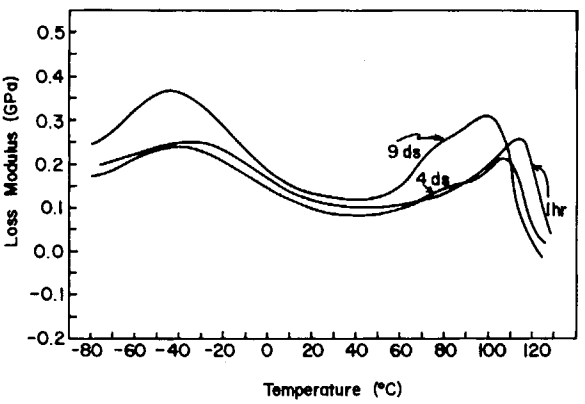

Fig. 6. Loss modulus (E'') as a function of temperature for formulation 1. The annealing times were 1 h, 4 days, and 9 days.

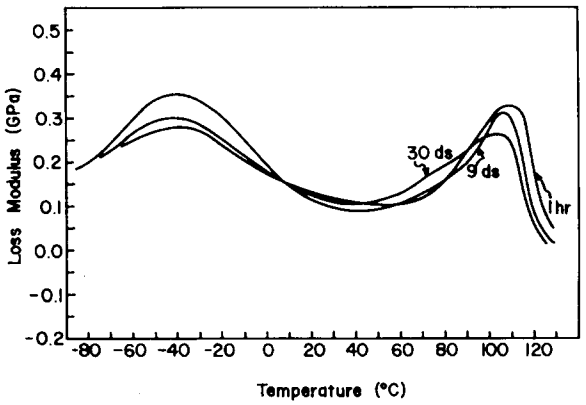

Fig. 7. Loss modulus (E'') as a function of temperature for formulation 2. The annealing times were 1 h, 9 days, and 30 days.

carefully controlled slow curing would minimize the formation of frozen-in stresses, but, in practice, such step is not always economically feasible.

The low temperature relaxation (T_β), which is believed to represent the onset of the crankshaft motion of the glyceryl group, was also found to decrease with annealing time, as shown in Figures 2–4. An explanation of this behavior is also offered in terms of the molecular rearrangements during annealing. As the frozen-in stresses are gradually relieved, the less hindered chains will display less difficulty in initiating the crankshaft motion and will do so at a relatively lower temperature. Hence, the onset of β relaxation will be shifted to a lower temperature.

Almost all fracture specimens exhibited an apparent cohesive [center of bond (COB)] failure, as shown in Figure 9. Occasionally, a crack was found to propagate (over a short distance) along the resin–metal interface, but such points were not considered for the calculations of strain energy release rate. The crack propagation path was observed to migrate between the aluminum adherends, although the fracture remained invariably within the adhesive. Each initiation occurred in a plane different from that in which the crack had arrested. Similar experimental results have also been reported by other researchers.[22,23] A recent

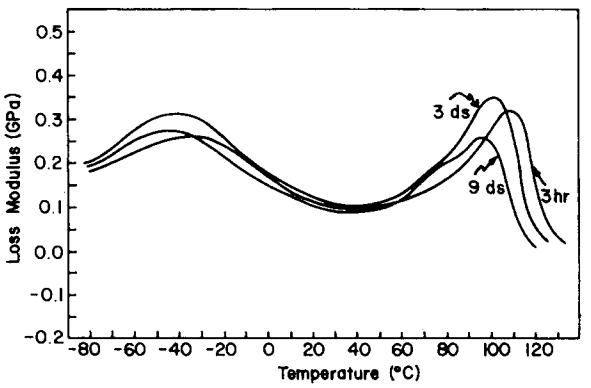

Fig. 8. Loss modulus (E'') as a function of temperature for formulation 3. The annealing times were 3 h, 3 days, and 9 days.

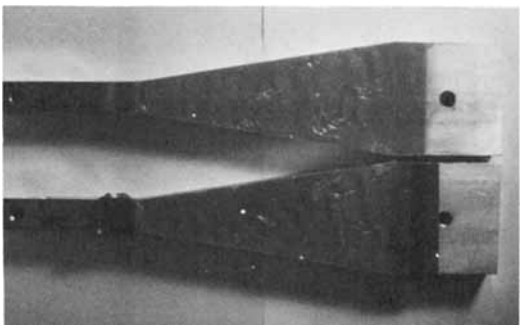

Fig. 9. A photograph of the fracture surface of formulation 2 annealed for 3 days.

analytical study of the effect of crack elevation in the height-tapered double cantilever beam (HTDCB) adhesive test configuration showed that the crack growth angle increases with respect to its original plane, as the crack approaches the adhesive–adherend interface.[24]

Quantitatively, the results of fracture measurements are presented in terms of

$$\Delta G_{Ic} = G_{Ic_i} - G_{Ic_a} \tag{1}$$

where ΔG_{Ic} represents the difference between the critical values of strain energy release rates for crack initiation (G_{Ic_i}) and crack arrest (G_{Ic_a}). The use of ΔG_{Ic} as a measure of the brittleness of a system has been discussed previously.[23] It follows directly from the classical Griffith criterion[25] that in ideally elastic materials, once initiated, a crack would propagate catastrophically through the entire specimen. In such a case, the total amount of energy stored in the beams would be spent entirely for the formation of new surfaces. Although in brittle thermosets a certain amount of plastic flow is associated with the formation and growth of cracks, the use of LEFM analysis is justified because of the small size of the zone in which nonlinear strains exist. As a consequence of this plastic flow, in most brittle thermosets cracks propagate in a slip-stick manner and the length of a crack jump is related to the sample brittleness. The larger the amount of plastic flow during initiation, the smaller the distance the crack propagates and consequently the smaller the ΔG_{Ic}. This is qualitatively shown in Figure 10 in which the load-deflection diagrams of two samples of different brittleness are compared.

In all three formulations, changes in fracture properties follow a similar pattern as a function of annealing time. The values of ΔG_{Ic} for filled systems (formulations 2 and 3) lie above those of the neat resin (formulation 1) as seen in Figure 11. The presence of the coupling agent appears to lead to a slight decrease in ΔG_{Ic}, as seen by comparing the fracture characteristics of formulations 2 and 3. Small changes observed within the first several hours are followed by a gradual decrease in ΔG_{Ic} at longer annealing times. This observed decrease in ΔG_{Ic} and hence the decrease in brittleness can also be accounted for in terms of the inhomogeneous thermoset morphology and molecular rearrangements during annealing. Samples annealed for a short time contain more frozen-in stresses due to a larger number of chains which are "trapped" and possess restricted (hindered) mobility. Hence, these chains (already strained) will account for *less*

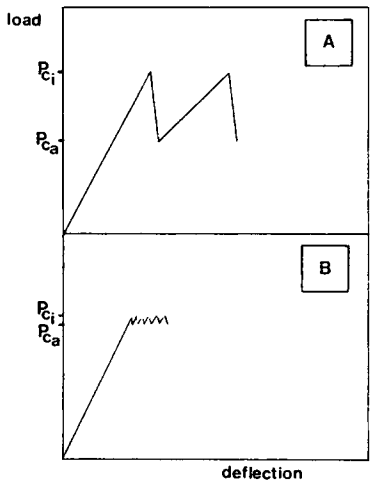

Fig. 10. A schematic of load-deflection curves for two epoxy resins. Sample A is more brittle than sample B and hence $(\Delta G_{Ic})_A > (\Delta G_{Ic})_B$.

plastic flow during the crack initiation and will appear more brittle (larger ΔG_{Ic}). As a consequence of molecular rearrangements during annealing, the frozen-in stresses are being gradually relieved, and the molecules are approaching their equilibrium conformations. Hence, during the application of load, these molecules will be capable of undergoing more plastic flow than the strained (hindered) chains, and, as a result, the sample brittleness (measured by ΔG_{Ic}) will decrease.

Finally, transmission electron microscope (TEM) was used to obtain TEM

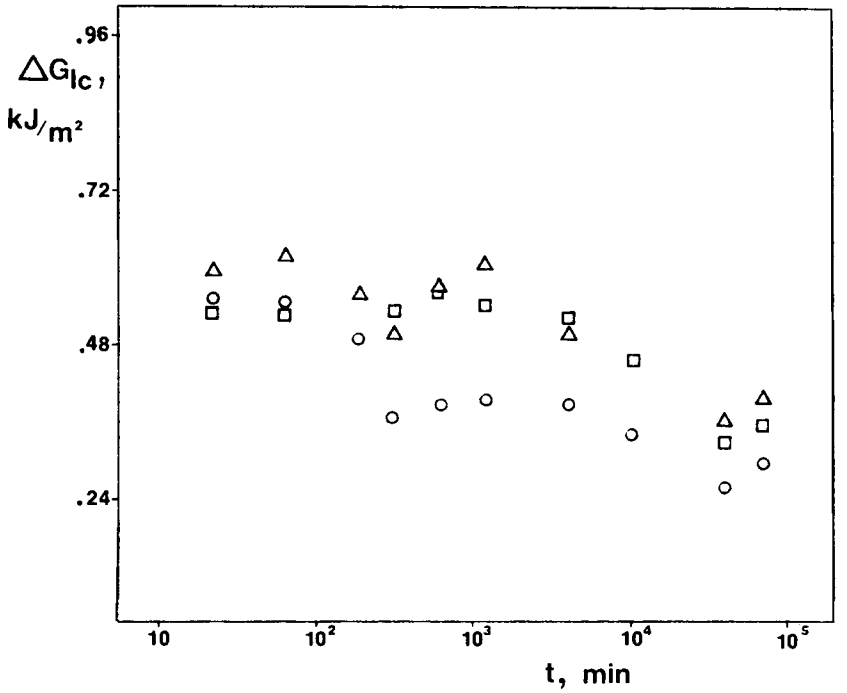

Fig. 11. ΔG_{Ic} as a function of annealing time for all three formulations: (○) 1; (△) 2; (□) 3.

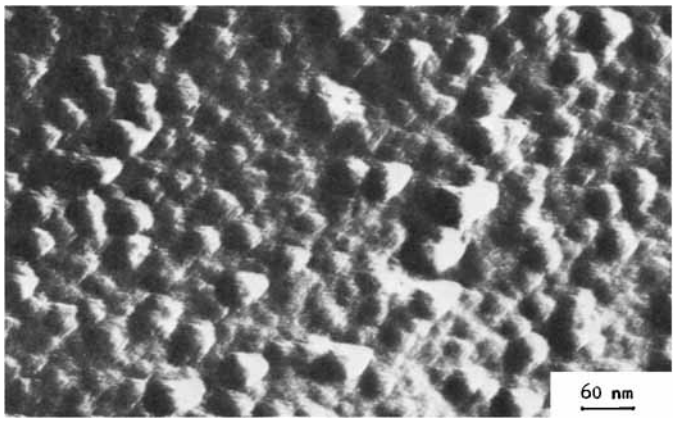

Fig. 12. Transmission electron micrograph of a one-stage C—Pt replica of fracture surface of formulation 1 annealed for 3 days.

photomicrographs of fracture surfaces of various samples. Each crack jump was characterized by the presence of three distinct zones on the fracture surface. The initiation and arrest zones were typified by the presence of ridges which are the consequence of local plastic flow and have been described previously.[20,23] Nevertheless, those zones were confined to a small length in comparison to the propagation zone, which appeared smooth to the naked eye but showed a characteristic nodular morphology under the microscope. One such TEM photomicrograph is shown in Figure 12. Fracture proceeds around the roughly spherical entities, indicating that these indeed are the sites of higher crosslink density in the system. Hence, the morphological model (composed of higher crosslink density regions immersed in a lower crosslink density matrix), which was used to explain changes in thermomechanical properties of crosslinked epoxies, is corroborated by the TEM study. Unfortunately, the relative scale of molecular rearrangements in the matrix during annealing precludes the observations of such changes in the electron microscope.

CONCLUSIONS

The effect of sub-T_g annealing on dynamic mechanical and fracture properties of various epoxy resin formulations was evaluated. A gradual decrease in glass transition as a function of annealing time was observed in all systems. After several days of annealing, a new relaxation (T_g') appears in the dynamic mechanical spectra. This relaxation is believed to have been caused by the molecular rearrangements in the epoxy resin network during annealing. An explanation for such rearrangements was offered in terms of the concept of inhomogeneous thermoset morphology. Electron-microscopic study corroborated the morphological model of higher crosslink density regions immersed in a lower crosslink density matrix.

Changes in fracture properties as a function of annealing time were followed by measuring ΔG_{Ic}. This parameter, in turn, provides information about the sample brittleness. A decrease in ΔG_{Ic} was observed at longer annealing times, and an explanation was again offered in terms of the model of inhomogeneous thermoset morphology.

The author is grateful to Mr. W. L. Chien, who performed most of the experimental work, Mr. C. D. Marshall (Shell Company, Houston), who supplied the resin, and Mr. R. Tong (American Cyanamid), who supplied the primer. Partial support of this study, provided by the Engineering Foundation, is gratefully acknowledged.

References

1. A. J. Kovacs, *J. Polym. Sci.*, **30** 131 (1958).
2. G. Pelistocker, *Kunststoffe*, **51**, 509 (1961).
3. G. Pelistocker, *Br. Plast.*, **35**, 365 (1962).
4. A. J. Kovacs, *Fortschr. Hochpolym.—Forsch.*, **3**, 394 (1963).
5. D. G. LeGrand, *J. Appl. Polym. Sci.*, **13**, 2129 (1969).
6. S. E. B. Petrie, *Bull. Am. Phys. Soc.*, **17**, 373 (1972).
7. S. S. Sternstein and T. C. Ho, *J. Appl. Phys.*, **43**, 4370 (1972).
8. S. E. B. Petrie, in *Polymeric Materials: Relationships between Structure and Mechanical Behavior*, E. Baer and S. V. Radcliffe, Eds., Am. Soc. for Metals, Metals Park, Ohio, 1975, Chap. 2.
9. S. Matsuoka, H. E. Bair, S. S. Bearder, H. E. Kern, and J. T. Ryan, *Polym. Eng. Sci.*, 18(14), 1073 (1978).
10. U. T. Kreibich and R. Schmid, *J. Polym. Sci., Polym. Symp.*, **53**, 177 (1975).
11. Z. Ophir, J. A. Emerson, and G. L. Wilkes, *J. Appl. Phys.*, **49**(10), 5032 (1978).
12. G. L. Wilkes, J. Dun, E. Kong, A. Banthia, and J. McGrath, *Polym. Prepr.*, **21**(2), 38 (1980).
13. J. Kaiser, *Makromol. Chem.*, **180**, 573 (1979).
14. J. Mijović, *J. Appl. Polym. Sci.*, **27**, 1149 (1982).
15. E. J. Ripling, S. Mostovoy, and H. T. Corten, *J. Adhesion*, **3**, 107 (1971).
16. J. Mijović and J. A. Koutsky, *J. Appl. Polym. Sci.*, **23**(4), 1037 (1979).
17. J. K. Gillham, *Polym. Eng. Sci.*, **19**(10), 676 (1979).
18. D.H. Droste and A. T. DiBenedetto, *J. Appl. Polym. Sci.*, **13**, 2149 (1969).
19. B. L. Lee and L. E. Nielsen, *J. Polym. Sci., Polym. Phys. Ed.*, **15**, 683 (1977).
20. J. Mijović and J. A. Koutsky, *Polymer*, **20**(9), 1095 (1979).
21. J. Mijović and L. Tsay, *Polymer*, **22**(7), 902 (1981).
22. S. Mostovoy, C. R. Bersch, and E. J. Ripling, *J. Adhesion*, **3**, 125 (1971).
23. J. Mijović, *J. Appl. Polym. Sci.*, **25**, 1179 (1980).
24. S. S. Wang, J. F. Mandell, and F. J. McGarry, Research Report R 76-3, MIT, 1976.
25. A. A. Griffith, *Phil. Trans. Roy. Soc. Lon., A*, **221**, 163 (1920).
26. G. R. Irwin, in *Treatise on Adhesion and Adhesives*, R. L. Patrick, Ed., Marcel Dekker, New York, 1967, Vol. 1, p. 223.

Received December 2, 1981
Accepted January 22, 1981